Appl Nanosci (2012) 2:275–283
DOI 10.1007/s13204-012-0104-x

ORIGINAL ARTICLE

Magnetoelectric and magnetodielectric properties of SBN–CMFO nanocomposites

S. R. Jigajeni · A. N. Tarale · D. J. Salunkhe · S. B. Kulkarni · P. B. Joshi

Received: 20 November 2011 / Accepted: 22 March 2012 / Published online: 7 April 2012

Abstract The paper reports synthesis of nanoparticles of $Sr_{0.5}Ba_{0.5}Nb_2O_6$ (SBN) and $Co_{1.2-x}Mn_xFe_{1.8}O_4$ (CMFO) via ceramic and hydroxide co-precipitation routes, respectively. The nanopowders of SBN–CMFO0.1 (MSBN0.1) and SBN–CMFO0.3 (MSBN0.3) are compacted together to form the desired magnetoelectric/magnetodielectric (ME/MD) composites. The Bi_2O_3 is used as a sintering aid. The Bi_2O_3 at three weight percent is observed to cause agglomeration of SBN and CMFO particles and improve the magnetomechanical coupling. The paper reports synthesis, structural and morphological studies on the MSBN composites. The composites are investigated for their dielectric, ME and MD properties. The results on the magnetocapacitance (MC) are observed interesting and could be correctly understood in terms of the stress-induced variation in the dielectric constant. The MC is observed to remain fairly constant between 10 and 500 kHz and possess a useful magnitude of nearly 4 %.

Keywords $(SrBa)Nb_2O_6$ · $(CoMn)_{1.2}Fe_{1.8}O_4$ · ME composites · Magnetocapacitance

Introduction

The composites of ferroelectric and magnetostrictive compounds are known to exhibit a useful magnitude of magnetoelectric coupling (Liu et al. 2009; Ostashchenko et al. 2008; Ma et al. 2008; Dong et al. 2008). The magnetoelectric effect in these composites is known to be due to stress-induced change in remanent polarization of the ferroelectric system in the magnetoelectric composites. Therefore, these composites need the presence of ferroelectric/relaxor composition possessing a useful value of maximum polarization (P_{max}), remanent polarization (P_r) and piezoelectric coefficient(d), while the magnetostrictive phase is required to possess a large value of resistivity (ρ), magnetostriction (λ) and low value of magnetocrystalline anisotropy energy, i.e., low value of coercive field H_c. As shall be seen in the next paragraph, the $Sr_{0.5}Ba_{0.5}Nb_2O_6$ (SBN) and Mn-substituted cobalt ferrite form a correct choice for the formation of such compositions (Chen and Tang Y 2004; Li et al. 2006). Further, recently the laminated magnetoelectric (ME) composites of PZT-$(MnZn)Fe_2O_4$ (MZF) are observed to exhibit useful magnitude of magnetodielectric coupling in the vicinity of electromechanical resonance frequency (Gridnev et al. 2009). This phenomenon was also attributed to the stress-induced change in polarization and therefore the dielectric constant. At present, the ME effect in such composites is better known but the magnetodielectric (MD) effect has rarely been investigated. Both the ME and MD effects in these systems are possible to be understood in terms of Landau thermodynamic theory as discussed by Zhong and Jiang (2008).

Most studies in the past focused on $CoFe_2O_4$, which was applied as one of the constituent of ME composites for its large magnetostriction (Boomgaard and Born 1978; Mahajan et al. 2002). However, the ME voltage coefficient was far smaller than the predicted value due to the poor ME coupling between the $CoFe_2O_4$ and ferroelectric phase probably due to the large anisotropy energy of the $CoFe_2O_4$. Here, substitution of Mn at A or B site is

A. N. Tarale · D. J. Salunkhe · P. B. Joshi (✉)
School of Physical Sciences, Solapur University, Solapur 413255, India
e-mail: drpbjoshi@rediffmail.com

S. B. Kulkarni
Department of Physics, Institute of Science, Mumbai, India

S. R. Jigajeni
Walchand Institute of Technology, Solapur 413006, India

observed to reduce the anisotropy energy and improve the magnetomechanical coupling of the $CoFe_2O_4$. Therefore, considering virtues of Co and Mn ions in the ferrite system, $Co_{1.2-x}Mn_xFe_{1.8}O_4$ (CMFO) has been selected as a piezomagnetic phase to form the ME/MD composites (Bhame et al. 2006, 2007; Caltun et al. 2007; Paulsen et al. 2005). As the physical properties of ferrites are dependent on the details of process of synthesis, initially the ferrite system CMFO is synthesized and investigated for its physical and magnetic properties viz. electrical resistivity (ρ), saturation magnetization (M_s), permeability (μ), coercive field (H_c) and coefficient of magnetostriction (λ) as a function of x varying between 0 and 0.4. For the present studies two ferrite compositions are selected, first $x = 0.1$ where λ is maximum but ρ is comparatively low and second $x = 0.3$ where λ is comparatively low but ρ is high.

Further, the relaxors ferroelectrics are known to have very large electrostrictive response in addition to the piezoelectric coupling; however, most relaxors contain Pb and their lack of remanent polarization makes them unsuitable for piezoelectric applications. An exception is the (Sr, Ba) Nb_2O_6 family which can sustain remanent polarization after polling. Therefore, investigations on ME and MD composites with $Sr_{0.5}Ba_{0.5}Nb_2O_6$ (SBN) as a piezoelectric phase are observed to be interesting (Chen and Tang Y 2004; Li et al. 2006).

Owing to the discussion above, the present paper reports synthesis and characterization of ME and MD composites yMSBN = yCMFO + (1−y) SBN + 3 % Bi_2O_3 w/w. The paper reports ME and MD properties of the above system for CMFO possessing $x = 0.1$ and 0.3. The parent composition CMFO and SBN are initially studied to confirm the formation of the required SBN and CMFO phases and particle size in nanometer range. The paper reports investigations on crystal structure, morphology, dielectric, linear magnetoelectric coefficients (α), quadratic magnetoelectric coefficient (β) and the magnetocapacitance (MC) defined through the relation $MC = ((\varepsilon(H)-\varepsilon(0))/\varepsilon(0)) \times 100$ %. MC is determined with applied magnetic field, H_{dc}, parallel and perpendicular to the applied ac electric field, E_{ac}. The dielectric properties are investigated as a function of temperature from 300 to 470 °K and frequency (f) between 100 and 1 MHz, while ME and MD properties are determined at room temperature as a function of f and H_{dc} up to 6 kOe. The variation of α, β and MC are studied as a function of f and sintering temperature T_s.

Experimental

Synthesis of CMFO

To achieve near atomic level uniformity of the constituents, the hydroxide co-precipitation route has been adopted for the synthesis of $Co_{1.2-x}Mn_xFe_{1.8}O_4$ (CMFO). The $Co(No_3)_2{\cdot}6H_2O$, $Fe(NO_3)_3{\cdot}9H_2O$ and $MnCl_2$ of AR grade are used as precursors for the hydroxide co-precipitation. The precursors are dissolved in distilled water to form nearly 40 mM solutions of the constituents and NH_4OH is used as precipitant. The precipitates are thoroughly washed in distilled water keeping alkaline medium using NH_4OH (pH 9) (Gang et al. 2003). The dried precipitates are calcined at 1,000 °C for 12 h, and final sintering is carried out at 1,200 °C for 24 h in two steps with intermediate grinding. The product of final sintering is formed as a powder and also pellets of 1 cm diameter. The powder has been used for the formation of magnetoelectric composites, while the pellets are used for determination of ρ, M_s, H_c and λ. To form a magnetoelectric composite, the requirement is a high value of ρ, Ms, μ, λ and a low value of H_c.

As discussed earlier, the CMFO is initially characterized for the determination of these parameters, and Table 1 shows variation of ρ, M_s, H_c, μ and λ as a function of x. The variations of physical parameters are consistent with the values reported earlier for CMFO system (Caltun et al. 2007). It could be seen that for $x = 0.1$ and 0.3, the parameters are optimum for its use as a magnetostrictive phase. For $x = 0.1$, λ is maximum but ρ is low and for $x = 0.3$, λ is comparatively low but ρ is high, and therefore the CMFO with $x = 0.1$ and 0.3 are selected as the magnetostrictive phase.

Synthesis of SBN

The SBN has been synthesized using standard ceramic route of synthesis because the precursors required for co-precipitation of niobium are not cost effective. High purity (>99.9 %) $BaCO_3$, $SrCO_3$ and Nb_2O_5 are used as precursors. Considering the earlier reports, pre-sintering and final sintering processes are carried out at 1,100 °C for 24 h, and 1,250 °C for 12 h, respectively, to form the fine-grained SBN powder (Pathak et al. 2004; Kulkarni et al. 2006). Due to pre-sintering and final sintering at 1,100 and 1,250 °C, respectively, it is observed that the SBN with the required TTB crystal structure and the required relaxor type of

Table 1 The variation of resistivity (ρ), saturation magnetization (M_s), permeability (μ), coercive field (H_c) and coefficient of magnetostriction (λ) for CMFO

$Co_{1.2-x}Mn_xFe_{1.8}O_4$ x	Resistivity (ρ)	M_s	H_c (Oe)	μ	λ
0.0	17.96×10^6	265	60	553.62	92
0.1	6.9×10^3	252	68	1,154	147
0.2	6.16×10^5	181	67.50	856.15	128
0.3	3.46×10^6	179	52.50	734.0	115
0.4	1.95×10^6	172	60	913.24	65

behavior, with a diffused phase transition (DPT) in the vicinity of 103 °C, is formed in the present case. These features are discussed in the fourth coming discussion of the paper.

Formation of composites

The resulting powders of CMFO and SBN are ground thoroughly to form uniform and submicron level particle size. The powders of CMFO and SBN thus formed are used to form the required ME/MD composites using the following formula

$$(y)\mathrm{CMFO0.1} + (1-y)\mathrm{SBN} + 3\ \%\ \mathrm{Bi_2O_3\ w/w} = (y)\mathrm{MSBN0.1}$$

$$(y)\mathrm{CMFO0.3} + (1-y)\mathrm{SBN} + 3\ \%\ \mathrm{Bi_2O_3\ w/w} = (y)\mathrm{MSBN0.3}$$

where 0.1 and 0.3 represents the contents of Mn in CMFO and $y = 0.3$, 0.4 and 0.5.

The composites above are termed as yMSBN0.1 and 0.3, respectively, during the course of further discussions. Considering the earlier reports, the composites are formed as pellet shaped samples of 1 cm diameter and three separate batches of the composites are formed with sintering temperature T_s equal to 1,100, 1,160 and 1,225 °C for yMSBN0.3 and two separate batches at T_s equal to 1,160 and 1,225 °C for yMSBN0.1. Three wt% of Bi_2O_3 is added as a sintering aid to facilitate the formation of large-grained composites at fairly low sintering temperature. This process may improve the possible magnetomechanical coupling of ME composites (Veer et al. 2008). Different sintering temperatures are used to understand the effect of sintering temperature on the dielectric and ME properties.

The HP4284A LCR-Q meter is used for the measurements of dielectric constant and complex impedance spectra. Custom built setups are used for the measurement of the ρ, the linear α and β at 850 Hz and variation of α with frequency up to 5 kHz (Salunkhe et al. 2008). To understand the crystal structure of the CMFO, SBN and MSBN composites, Bruker D8 advance XRD spectrometer has been used, while the SEM pictures are obtained using JEOL JSM-6360 SEM.

Results and discussion

The individual powders of the ferrite and the ferroelectric materials are investigated for structural studies for confirmation of the formation of the desired phase and the estimation of the particle size. The XRD spectrum of CMFO is shown in Fig. 1. The reflections are in confirmation with the JCPD data on cobalt ferrite possessing cubic spinel

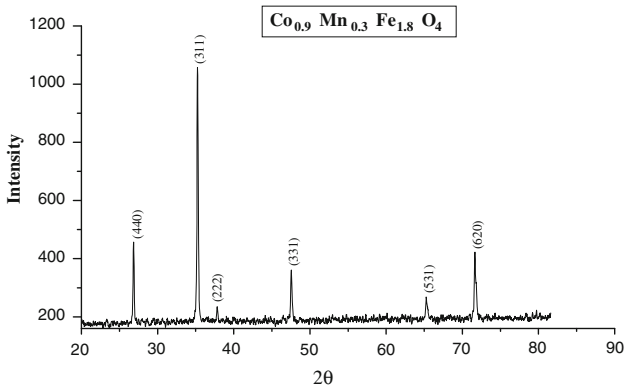

Fig. 1 XRD spectra of $Co_{0.9}Mn_{0.3}Fe_{1.8}O_4$ (CMFO)

crystal structure, with lattice parameter 'a' equal to 8.20 Å, which is in confirmation with earlier reports (Bhame et al. 2006, 2007). Further, the XRD spectra showed that no peak corresponding to any impurity phase occurs; thus, it could be concluded that the CMFO powder of required spinel crystal structure is formed in the present case. Using the Scherrer formula, the particle size of CMFO powder is estimated to be 52 nm.

Figure 2 shows the XRD spectra of SBN powder which shows the reflections corresponding to TTB crystal structure and the spectra is in confirmation with the earlier reports. The particle size of SBN is observed to be 35 nm as determined using Scherrer formula (Jigajeni et al. 2010). The parameters 'a' and 'c' determined from the XRD spectra are $a = b = 5.97$ Å and $c = 2.46$ Å, respectively (Jigajeni et al. 2010).

Figures 3 and 4 show the XRD spectra of composites for 0.4MSBN sintered at 1,100 and 1,160 °C, respectively. The peaks corresponding to SBN and CMFO are separately identified in the XRD spectra of composites. The XRD spectra for remaining composites with y between 0.3 and 0.5 and for the sintering temperatures 1,100, 1,160 and 1,225 °C are similar to the XRD spectra as shown in

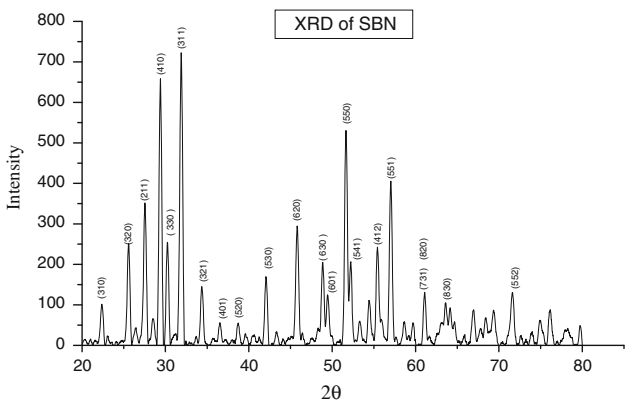

Fig. 2 XRD spectra of $Sr_{0.5}Ba_{0.5}Nb_2O_6$ (SBN)

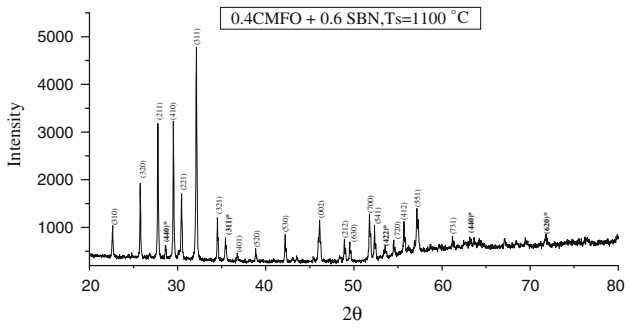

Fig. 3 XRD spectra of *y*MSBN0.3 composite, $y = 0.4$ sintered at 1,100 °C

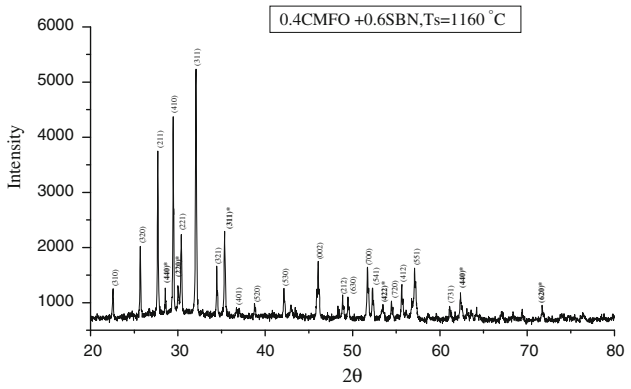

Fig. 4 XRD spectra of *y*MSBN0.3 composite $y = 0.4$, sintered at 1,160 °C

Table 2 Variation of relative intensities of (311) planes of CMFO and SBN sintered at 1,160 °C, *y*MBSN0.3

y	I_{CMFO}/I_{SBN}
0.3	0.25
0.4	0.44
0.5	0.51

Figs. 3 and 4. To determine the correlation between the variation of relative intensity of the individual phases of CMFO and SBN, the ratio of relative intensities of highest intensity peaks of CMFO and SBN is determined as a function of y. Table 2 shows variation of ratio of relative intensities I_{CMFO}/I_{SBN} corresponding to (311) reflection of CMFO and SBN, respectively. From the table, it is observed that the relative intensity of (311) reflections of the ferrite phase increases monotonically with increasing y. This feature could be correlated to increasing content of CMFO with y. Thus, the above observation indicates that pure biphase composites are formed in this process.

Microstructure

Figure 5a–c show the SEM photographs for the composites 0.4MSBN0.3 sintered at 1,100, 1,160 and 1,225 °C, while Fig. 5d shows SEM photograph for 0.4MSBN0.3 sintered at 1,160 °C. All images show the formation of aggregates of the individual phases grown up to 4 μm due to addition of the Bi_2O_3 as a sintering aid (Veer et al. 2008).

Dielectric properties

Figure 6 shows variation of ε at 1 kHz as a function of T for the SBN and MSBN series. It could be seen that the ε versus T behavior shows a DPT at 103 °C. This DPT corresponds to the signature of DPT of SBN at $T_c = 103$ °C (Pathak et al. 2004). Another interesting observation of ε versus T behavior is that the ε increases with T in paraelectric region above DPT. The increase in the ε is faster for increasing y. This feature is known to occur because of interfacial polarization occurring at boundaries between the SBN and CMFO phases due to difference in the resistivity (Jigajeni et al. 2010). Interfacial polarization is known to be prominent at higher frequencies and increases as T increases. The present observation suggests that the increase in ε in the paraelectric region appear to be due the presence of interfacial polarization.

To investigate this feature further, the ε versus T behavior is determined as a function of f for all the compositions. Figure 7 shows variation of dielectric constant as a function of frequency of composite 0.4MSBN0.3 sintered at 1,225 °C. The behavior for other values of y is similar to those in Fig. 7. The frequency is varied between 100 and 1 MHz and the figure shows a DPT at 103 °C corresponding to the SBN phase. In this case also, as reported earlier, after the DPT, the ε increases with temperature in the paraelectric region above T_c, the increase in ε is faster for lower frequencies as compared to the higher ones. Therefore, it could be seen that the dielectric constant of the composite consists of two contributions: one due to the ferroelectric contribution of SBN and the other due to the presence of interfacial polarization at the boundaries between SBN and CMFO phases (Jigajeni et al. 2010).

Table 3 shows variation of ε and Q at room temperature and T_c, respectively, for the MSBN0.3 series. From the table, it is observed that the dielectric constant ε at room temperature decreases with increase in y.

Magnetoelectric effect

The dynamic ME coefficient $\alpha = dv/(dH \times d)$ and $\beta = dv/(dH \times 2ho)$ of the composites is measured at 850 Hz using a custom-designed measurement unit (Salunkhe et al. 2008). Here v is the rms ac voltage developed across the sample in response to rms ac magnetic field H and d is the length of the sample.

Figure 8 shows variation of α as a function of y for the MSBN0.3 composites sintered at 1,100, 1,160 and 1,225 °C, respectively, while the Table 4 shows variation

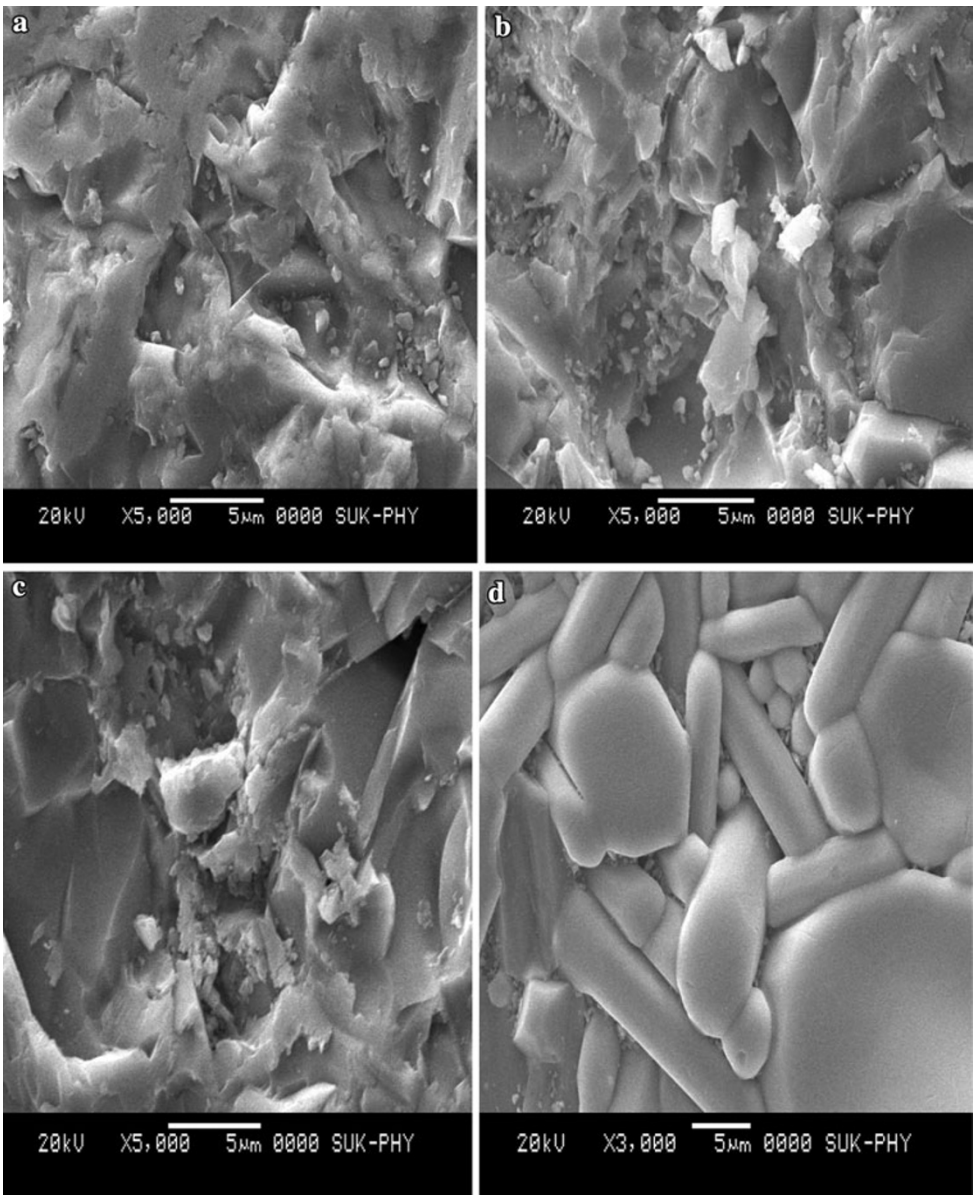

Fig. 5 **a–c** SEM picture for 0.4MSBN0.3 for 1,100, 1,160 and 1,225 °C, respectively, and **d** for 0.4MSBN0.3 for $T_s = 1{,}160$ °C

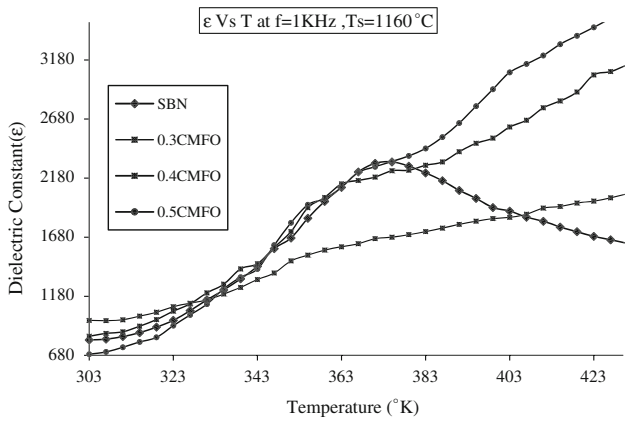

Fig. 6 Variation of ε with temperature at $f = 1$ kHz for SBN and *y*MSBN0.3 composites sintered at $T_s = 1{,}160$ °C

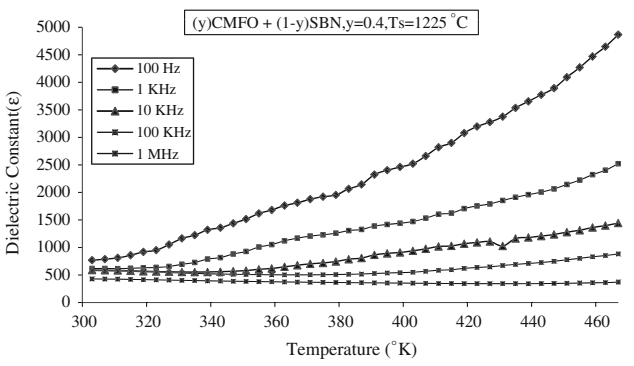

Fig. 7 Variation of ε with temperature of *y*MSBN0.3 composite $y = 0.4$ sintered at 1,225 °C

Table 3 Variation of dielectric constant ε and Q at 1 kHz for the composites yMBSN0.3 sintered at 1,160 °C

y	ε at room temperature	Q at room temperature	ε at 106 °C	Q at 106 °C
0.3	975.77	4.28	1,701.7	3.68
0.4	841.7	3.22	2,246.9	1.87
0.5	689.69	2.57	2,368.2	1.28

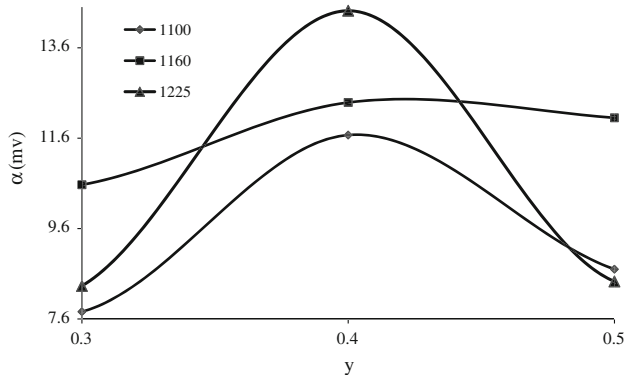

Fig. 8 Variation of α with y for MSBN0.3 composites sintered at 1,100, 1,160 and 1,225 °C

of α with y. The α is observed to increase for increasing sintering temperature, which could be attributed to the increased grain size and resulting improved magnetomechanical coupling. This feature too is similar to observations on nickel ferrite and PZT systems (Shrinivasan et al. 2001); α is observed to pass through a broad maximum for $y = 0.4$. This feature is attributed to the $y \times (1-y)$ type of proportionality of α in the case of biphase composite system. Further, the magnitude of α is known to be proportional to $(\lambda \times k_m \times d)/\varepsilon$ where λ is coefficient of magnetostriction, k_m is magnetomechanical coefficient, d is piezoelectric constant and ε is dielectric constant. From the SEM pictures (Fig. 5a–d), it is revealed that the agglomeration of the SBN and CMFO particles occurred in the case of y MSBN0.3 systems. The agglomeration may increase with T_s and the magnitude of k_m and therefore α increase as a function of sintering temperature as seen in Table 4. This is evident from the magnitude of $\alpha = 14.49$ mv/Oe/cm for 0.4MSBN0.3 at $T_s = 1{,}225$ °C. This shows the usefulness of Bi_2O_3 in forming the composites.

Further, Fig. 9 shows the variation of α as a function of log f for $T_s = 1{,}160$ °C. The observations for other sintering temperatures are similar to the behavior in Fig. 9. As discussed above, α is inversely proportional to ε and as ε is observed to decrease with f, α is expected to increase with f. The present observations are similar.

To determine the magnitude of β, the ME output (v) is measured as a function of applied dc magnetic field, H_{dc}, between 0 and 4.5 kG. It is observed that as y increases the v increases with H_{dc}. This is expected from the proportionality of ME output v with λ. The λ is known to follow the variation of M_s with H_{dc}. As λ increases with H_{dc}, the ME output should also increase with H_{dc} as observed in the present case. Table 4 also shows the variation of β as a function of y. From Table 4, it is seen that similar to the variation of α, β also becomes maximum for $y = 0.4$. α and β both are expected to follow the relation $y \times (1-y)$ and the present observation of β confirm this prediction. α and β both pass through a broad maxima at $y = 0.4$, nearly equal to $y = 0.5$ as expected for the relation above.

Though α increases for increase in sintering temperature, β on the other hand becomes maximum for $T_s = 1{,}160$ °C. It is expected that this feature could be reflected in the magnitude of magnetocapacitance as shall be discussed in the next paragraphs.

Table 5 shows the variation of α and β as a function of y and T_s for yMSBN0.1 composites. From Tables 4 and 5, it could be seen that for the composites yMSBN0.1 and 0.3, the magnitude of α is nearly same but β increases in magnitude. The increased value of β may lead to an increase in the value of magnetocapacitance. Also, the α for $T_s = 1{,}225$ °C is observed to decrease with increase in y at the cost of β increasing from 5×10^{-4} to 20×10^{-4} mv/Oe^2/cm for y increasing from 0.3 to 0.5.

Figure 10 shows the variation of tan δ as a function of frequency and applied magnetic field. tan δ passes through

Table 4 Variation of linear and quadratic magnetoelectric coefficient α and β with y for the yMBSN0.3 composites sintered at 1,100, 1,160 and 1,225 °C

y	α (1,100 °C) mv/Oe/cm	α (1,160 °C) mv/Oe/cm	α (1,225 °C) mv/Oe/cm	β (1,100 °C) $\times$ 10^{-4} mv/Oe^2/cm	β (1,160 °C) $\times$ 10^{-4} mv/Oe^2/cm	β (1,225 °C) $\times$ 10^{-4} mv/Oe^2/cm
0.3	7.76	10.569	8.33	0.37	2.39	1.0
0.4	11.67	12.39	14.42	3.15	3.01	2.0
0.5	8.7	12.05	8.43	0.966	2.40	0.4

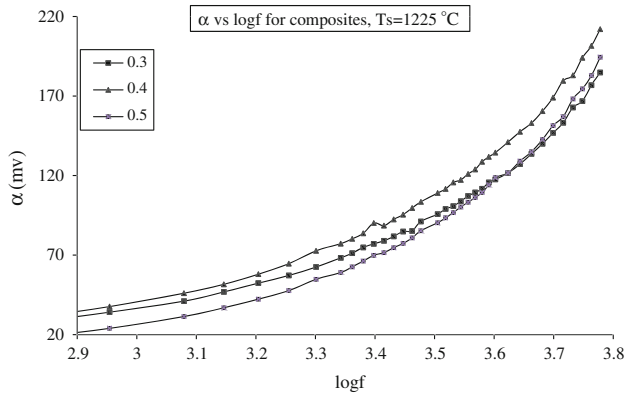

Fig. 9 Variation of α with log *f* for MSBN0.3 composites sintered at $T_s = 1{,}225$ °C

Table 5 Variation of linear and quadratic magnetoelectric coefficient α and *β* with y for the composites y MBSN0.1 sintered at 1,160 and 1,225 °C

y	α (1,160 °C) mv/Oe/cm	α (1,225 °C) mv/Oe/cm	*β* (1,160 °C) (mv/Oe^2/cm) × 10^{-4}	*β* (1,225 °C) (mv/Oe^2/cm) × 10^{-4}
0.3	7.6	12.2	20	5
0.4	14.0	10.5	8	10
0.5	14.3	6.6	5	20

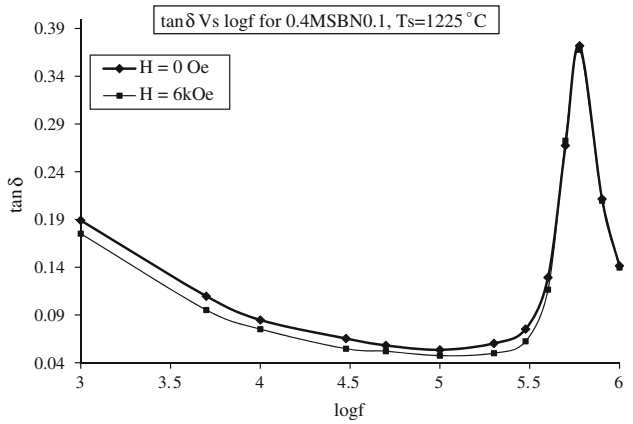

Fig. 10 Variation of tan *δ* with log *f* with applied magnetic field, H_{dc}, for MSBN0.1 composites sintered at 1,225 °C

a maximum for a frequency just above 500 kHz, which is expected to be the EMR resonance frequency for the radial mode of oscillations. It is also observed that the EMR frequency is independent of variations of *y*, *x* and T_s. This is expected because all the samples investigated possess diameter at 1.2 cm.

Interesting observations are on the variations of dielectric constant (*ε*) as a function of applied field, i.e., the MD behaviour. Figure 11 shows the variation of *ε* as a function

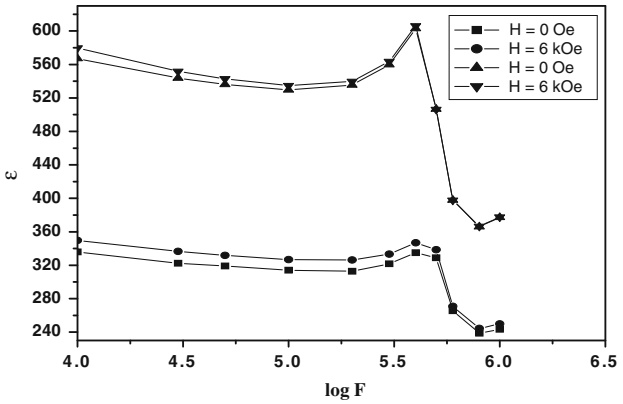

Fig. 11 The variation of *ε* with log *f* and applied magnetic field, H_{dc}, for *y*MSBN0.3 and *y*MSBN0.1

of applied frequency (*f*) and applied magnetic field (H_{dc}) for *y*MSBN0.3 and 0.1. In the present case, the MC is determined in the two separate configurations of applied magnetic field and applied ac electric field (E_{ac}). In case one, the H_{dc} as well as E_{ac} are along the axis of disc, while in case two, H_{dc} is along the radius of disc and E_{ac} is along the direction of disc axis. Figure 11 represent the observations of case one. The variation of *ε* for other composition and sintering temperature T_s are similar in nature as shown in Fig. 11. Table 6 shows the variation of MC as a function of T_s both for case one and case two for *y*MSBN0.1 and frequencies $f = 10$ and 500 kHz, respectively. Further, Table 7 shows variation of MC as a function of *y*, T_s and for frequencies 10 and 500 kHz, respectively. It is observed that the MC in case one is large as compared to case two; therefore, only the variation of case one is recorded for *y*MSBN0.3.

As a part of discussion on MC, it is interesting to note the following behaviour. As discussed earlier, the MC occurs due to variation of dielectric constant because of the applied stress occurring due to the piezomagnetic effect in the ferrite phase (Gridnev et al. 2009). Further, the MC should be proportional to $\lambda \times k_m \times (d\varepsilon/ds)$, where *λ* is magnetostrictive coefficient, k_m the magnetomechanical coupling coefficient, $d\varepsilon/ds$ the rate of change of dielectric constant as a function of applied stress. For *λ* being positive, the stress would increase with increase in H_{dc}, while for *λ* negative stress would decrease with increase in H_{dc} and, therefore, *ε* increases with H_{dc}.

As discussed by Gridnev et al. (2009), the increase in stress will cause increase in P_{max} and, therefore, the *ε* decreases for increase in stress and vice versa. As *ε* decreases for increase in stress, the MC will be negative for positive *λ* and positive for negative *λ*. Further, it is already reported and discussed that the $\lambda_{\parallel}$ (parallel) is negative for CFMO composition, while $\lambda_{\perp}$ (perpendicular) is positive (Bhame et al. 2006, 2007). Also, it is observed that $\lambda_{\perp}$ is almost double that

Table 6 Magnetocapacitance (MC) for *y*MBSN0.1

y	MC (1,160 °C) %				MC (1,225 °C) %			
	Parallel		Perpendicular		Parallel		Perpendicular	
	10 kHz	500 kHz	10 kHz	500 kHz	10 kHz	500 kHz	10 kHz	500 kHz
0.3	2.2	1.2	−0.9	−0.3	0.5	0.15	−0.76	−0.3
0.4	0.17	0	−0.13	−0.1	4.2	3.1	−0.8	−0.5
0.5	0.45	0.14	−0.35	−0.01	2.2	1.2	−0.8	−0.6

Table 7 Magnetocapacitance (MC) for *y*MBSN0.3

y	MC (1,100 °C) %		MC (1,160 °C) %		MC (1,225 °C) %	
	Parallel		Parallel		Parallel	
	10 kHz	500 kHz	10 kHz	500 kHz	10 kHz	500 kHz
0.3	0.35	0.18	0.86	0.4	0.16	0
0.4	0.55	0.5	1.2	0.2	0.9	0.08
0.5	0.4	0.04	0.6	0.2	0.93	0.51

of $\lambda_{\|}$. As a conclusion to the above discussion, it is expected that in the case of case one, where H_{dc} is parallel with E_{ac}, $\lambda_{\|}$ will play its role in the determination of MC, i.e., as H_{dc} increases the stress reduces and ε increases, and MC is positive. Inverse will be the situation for case two and MC is negative. It is also expected that $MC_{\|}$ (parallel) should be almost double of $MC_{\perp}$ (perpendicular) as a product of the comparative magnitude of $\lambda_{\|}$ and $\lambda_{\perp}$.

The present observations are in confirmation with the qualitative logic as discussed in the above paragraph. MC is positive for case one while it is negative for case two. Also, magnitude of $MC_{\|}$ is sufficiently large as compared to $MC_{\perp}$. As a part, variation of MC with *y*, it is seen that α is maximum for $y = 0.4$ probably due to $y \times (1-y)$ relationship for the ME compositions. Further, it is also observed that the MC increases for increasing β. From Table 5, it is seen that for *y*MSBN0.1, the β is high for $T_s = 1.225$ °C as compared to $T_s = 1{,}160$ °C. Therefore, the MC should become maximum for $T_s = 1{,}225$ °C and $y = 0.4$. The present observations are in confirmation with the logic mentioned above. The magnitude of MC is significant in the present case that is at 4.2 %. Further, it is observed that unlike the MC due to the variation of interfacial polarization, the strain-induced MC in the present case is fairly large even up to the EMR frequencies at nearly 500 kHz (Catalan 2006).

Conclusions

It is observed that the Mn substitution at A-site in $Co_{1.2-x}Mn_xFe_{1.8}O_4$ causes the coefficient of magnetostriction (λ) to increase for x up to 0.1 only, though the overall value of λ remained more than that of cobalt ferrite for x up to 0.3. It is observed that the samples with $x = 0.1$–0.3 are useful to form piezomagnetic phase of the ME composites. Further, the nanoparticles of the CMFO as well as SBN could be produced via hydroxide co-precipitation and ceramic routes of synthesis, respectively, as detailed in the paper. The Bi_2O_3 is observed to cause densification of composites and leads to a substantial increase in the quality factor Q, ME coefficient α and magnetocapacitance (MC) of the MSBN composites. The observations on MC are promising and the results could be understood in terms of Landau thermodynamic theory. The MC has been observed to remain fairly constant for MSBN0.1 over a wide range of frequencies between 10 and 500 kHz. Also, the magnitude of MC is sufficiently large for 0.4MSBN0.1. The present observation suggest that further studies on ME composites are required to evolve compositions possessing useful value of ME and MD properties.

Acknowledgments The author hereby acknowledges with thanks the help rendered by Dr. Mukul Gupta, UGC–DAECSR, Indore (Madhya Pradesh), India, for acquisition of XRD data.

References

Bhame SD, Joy PA (2006) Enhanced magnetostrictive properties of Mn substituted cobalt ferrite $Co_{1.2}Fe_{1.8}O_4$. J Appl Phys 99: 073901

Bhame SD, Joy PA (2007) Magnetic and magnetostrictive properties of manganese substituted cobalt ferrite. J Appl Phys 40:3263

Boomgaard JVD, Born RAJ (1978) A sintered magnetoelectric composite material $BaTiO_3$–$Ni(Co,Mn)Fe_2O_4$. J Mater Sci 13: 1538

Caltun O, Chiriac C, Lupu N, Dumitru I, Rao BP (2007) High magnetostrictive doped cobalt ferrite. J Optoelectron Adv Mater 9:1158

Catalan G (2006) Magnetodielectric effect without multiferroic coupling. Appl Phys Lett 88:102902

Chen XM, Tang YH (2004) Dielectric and magnetoelectric characterization of CoFe2O4/$Sr_{0.5}Ba_{0.5}Nb_2O_6$ copmosites. J Appl Phys 96(11):6520–6522

Dong XW, Wu YJ, Wan JG, Wei T, Zhang ZH, Chen S, Yu H, Liu JM (2008) Phase shift of electric-field-induced magnetization in magnetoelectric laminate composite. J Phys D Appl Phys 41:035003. doi:10.1088/0022-3727/41/3/035003

Gang Xu, Weng Wenjian, Yao Jianxi, Piyi Du, Han Gaorong (2003) Low temperature synthesis of lead zirconate titanate powder by hydroxide co-precipitation. Microelectron Eng 66:568–573

Gridnev SA, Kalgin AV, Chernykh VA (2009) Magnetodielctric effect in two-layer magnetoelectric PZT–MZF composite. Integr Ferroelctr 109:70–75

Jigajeni SR, Kulkarni SV, Kolekar YD, Kulkarni SB, Joshi PB (2010) $Co_{0.7}Mg_{0.3}Fe_{2-x}Mn_xO_4$–$Sr_{0.5}Ba_{0.5}Nb_2O_6$ magnetoelectric composites. J Alloy Compd 492:402–405

Kulkarni AR, Patro PK, Harendranath CS (2006) Explaining the effect of homogeneity on microstructure, dielectric and ferroelectric properties of strontium barium niobate. In: Proceedings of NSAE 2006, pp 55–64

Li YJ, Chen XM, Lin YQ, Tang YH (2006) ME effect of $Ni_{0.8}Zn_{0.2}Fe_2O_4/Sr_{0.5}Ba_{0.5}Nb_2O_6$ composites. J Eur Ceram Soc 26(13):2839–2844

Liu M, Obi O, Lou J, Stoute S, Cai Z, Ziemer K, Sun NX (2009) Strong magnetoelectric coupling in ferrite/ferroelectric multiferroic heterostructures derived by low temperature spin-spray deposition. J Phys D Appl Phys 42:045007. doi:10.1088/0022-3727/42/4/045007

Ma J, Gong Shi Z, Nan CW (2008) Magnetic-field induced electric response of simple magnetoelectric composite rods. J Phys D Appl Phys 41:155001. doi:10.1088/0022-3727/41/15/155001

Mahajan RP, Patankar KK, Kothale MB, Chaudhari SC, Mathe VL, Patil SA (2002) ME effect in cobalt ferrite–barium titanate composites and their electric properties. Pramana J Phys 58:1115–1124

Ostashchenko YuA, Preobrazhenskii VL, Pernod P (2008) Magnetoelectric effect in an asymmetric layered magnet-piezoelectric structure. Phys Solid State 50:463–468

Pathak MP, Patro PK, Kulkarni AR (2004) Dielectric properties of strontium barium niobate synthesized by Pechini method. In: Proceedings of NSFD XIII, vol 9, pp 206–210

Paulsen JA, Ring AP, Lo CCH (2005) Manganese-substituted cobalt ferrite magnetostrictive materials for magnetic stress sensor applications. J Appl Phys 97:044502

Salunkhe DJ, Veer SS, Kulkarni SV, Kulkarni SB, Joshi PB (2008) Experimental setup for the measurement of magneto-electric susceptibilities for different composites. J Inst Soc India 38(4): 294

Shrinivasan G, Rasmussen ET, Gallegal J, Shrinivasan R (2001) Magnetoelectric bilayer and multilayer structures of magnetostrictive and piezoelectric oxides. Phys Rev B 64:214408

Veer SS, Salunkhe DJ, Kulkarni SV, Joshi PB (2008) Effect of sintering aid on physical and magnetoelectric properties of $La_{0.7}Sr_{0.3}MnO_3$–$BaTiO_3$. Indian J Eng Mater Sci 15:121–125

Zhong CG, Jiang Q (2008) Theory of the magnetoelectric effect in multiferroic epitaxial $Pb(Zr_{0.3}Ti_{0.7})O_3/La_{1.2}Sr_{1.8}Mn_2O_7$ heterostructures. J Phys D Appl Phys 41:115002. doi:10.1088/0022-3727/41/11/115002